Environmetrics 00, 1–15

DOI: 10.1002/env.XXXX

Accepted for publication September 2018

A model for the directional evolution of severe ocean storms

S. Tendijck[a], E. Ross[b], D. Randell[b] and P. Jonathan[c,d*]

Summary: We develop a non-stationary Markov extremal model (MEM) as an extension of Winter and Tawn (2016, 2017) and use it to characterise the time evolution of extreme sea state significant wave height (H_S) and storm direction in the vicinity of the storm peak sea state. The approach first requires transformation of H_S from physical to standard Laplace scale, achieved using a non-stationary directional marginal extreme value model. The evolution of Laplace-scale H_S is subsequently characterised using a MEM, and that of the rate of change of storm direction described by an autoregressive model, the evolution variance of which is H_S-dependent. Simulations on the physical scale under the estimated model give realistic realisations of storm trajectories consistent with historical data for storm trajectories at a northern North Sea location.

Keywords: Extreme; Significant wave height; Storm trajectory; Markov extremal model; Non-stationary.

1. INTRODUCTION

We are often interested in understanding the evolution of time-series of extreme values, potentially non-stationary with respect to covariates. For example, in an oceanographic setting, there is interest in understanding the evolution of a severe ocean storm, consisting of a set of consecutive sea states, in time from sea state to sea state. This involves joint modelling of multivariate time-series of a combination of variables, some of which (e.g. sea state significant wave height, henceforth H_S for brevity) are extreme, and others (e.g covariates such as sea state storm direction) which are not. Such a model is important for reliable design of marine structures, enabling estimation of distributions of variables such as

[a] *Technical University of Delft, 2600 AA Delft, Netherlands.*
[b] *Shell Global Solutions International B.V., 1031 HW Amsterdam, Netherlands.*
[c] *Shell Research Ltd., London SE1 7NA, United Kingdom.*
[d] *Department of Mathematics and Statistics, Lancaster University LA1 4YW, United Kingdom.*
[*] *Correspondence to: philip.jonathan@shell.com*

This paper has been submitted for consideration for publication in *Environmetrics*

crest elevation, individual wave height and total water level for whole storm events consisting of multiple dependent sea states (as opposed to estimates for isolated sea states) given storm peak characteristics. These can then be combined with distributions for the statistics of storm peak magnitudes and storm rates of occurrence to estimate design conditions for return periods of arbitrary length, as explained e.g. in Feld et al. (2018). Such a model also allows the "directional dissipation" of an ocean storm to the characterised, facilitating consistent estimation of return values across directional sectors (e.g. Ross et al. 2017).

In the context of characterising heatwave evolution, Winter and Tawn (2016, 2017) introduce a Markov extremal model (`MEM`) for an interval of extreme values of time-series (transformed to standard Laplace marginal scale) motivated by the conditional extremes model of Heffernan and Tawn (2004). In this work we present a non-stationary extension of Winter and Tawn incorporating evolution of sea state H_S and direction. In outline, the approach consists of the following steps: (a) A common directional marginal model based on Ross et al. (2017) is established for H_S of all sea states of all storms, given direction; (b) The marginal model is used to transform the values of H_S given direction to standard Laplace scale using the probability integral transform; (c) Intervals of time-series of threshold exceedances of Laplace-scale H_S (of different lengths, but including occurrence of the storm peak, H_S^{sp}) and corresponding storm direction (together referred to as "storm trajectories") are isolated, for each of a large number of storm events; (d) A Markov extremal model of appropriate order is estimated to describe the evolution of Laplace-scale H_S relative to the storm peak; (e) An autoregressive time-series model of appropriate order with heterogeneous evolution variance dependent on Laplace-scale H_S is established for the rate of change of storm direction on its trajectory; (f) Models from steps (a), (d) and (e) are coupled to facilitate simulation of realistic storm trajectories on physical scale. The method developed here is motivated by ocean engineering requirements regarding characterisation of storm evolution, but is generally applicable to non-stationary time-series of extreme events such as precipitation, wind, ocean current (including features such as solitons) and storm surge in an environmental context.

The key idea behind the proposed approach is the conditional extremes model of Heffernan and Tawn (2004). This model is advantageous for two main reasons. (a) It allows effortlessly the characterisation of more general forms of extremal temporal and spatial dependence (including both asymptotic dependence and asymptotic independence) compared with its

main competitors based on max-stable process modelling (e.g. Padoan et al. 2010, Chavez-Demoulin and Davison 2012, Davison et al. 2012, Huser and Davison 2014) which typically admit only asymptotic dependence, although extensions to asymptotic independence, and mixtures of asymptotic dependence and asymptotic independence have been proposed (e.g. Wadsworth et al. 2017; Rootzen et al. 2018). (b) It allows the partitioning of large spatio-temporal problems into small pairwise ones. This facilitates computationally-efficient inference, including incorporation of the effects of covariates compared with competitors based on max-stable processes (but see also computationally elegant hierarchical max-stable models of Stephenson 2009; Reich and Shaby 2012.)

The layout of the article is as follows. A motivating application is given in Section 2, involving estimation of trajectories of extreme sea state H_S and corresponding storm direction for a location in the northern North Sea. Section 3 provides a description of the model. Application of the model to the northern North Sea example is then outlined in Section 4. A discussion of results and conclusions is provided in Section 5. The method by which distributions of `MEM` residuals are estimated is outlined in the appendix.

2. MOTIVATING APPLICATION

Significant wave height H_S can be defined as four times the standard deviation of the ocean surface elevation at a spatial location for a specified period of observation. The application sample is taken from the hindcast of Reistad et al. (2011), which provides time-series of significant wave height and (dominant) wave direction for three hour sea states for the period September 1957 to December 2012 at a northern North Sea location. Extreme sea states in the North Sea are dominated by winter storms originating in the Atlantic Ocean and propagating eastwards across the northern part of the North Sea. Sea states at northern North Sea locations are usually more intense than in the southern North Sea. Directions of propagation of extreme seas vary considerably with location, depending on land shadows of the British Isles, Scandinavia, and the coast of mainland Europe, and fetches associated with the Atlantic Ocean, Norwegian Sea, and the North Sea itself. In the northern North Sea the main fetches are the Norwegian Sea to the North, the Atlantic Ocean to the west, and the North Sea to the south. Extreme sea states from the directions of Scandinavia to the east and the British Isles to the south-west are not possible. The shielding by these land

masses is more effective for southern North Sea locations, resulting in a similar directional distribution but reduced wave heights by comparison with northern North Sea locations.

With θ indicating the direction from which waves propagate measured clockwise from North, Figure 1(a) shows a directional plot of the complete sample of H_S data in grey. Storm peak occurrences H_S^{sp} shown in black are local maxima of storm trajectories estimated as outlined in Section 3. The effect of the land shadow of Norway in particular is visible at $\approx 220°$. Figure 1(b) gives a polar plot of storm trajectories for 15 typical storms. The lengths and directional characteristics of storm trajectories vary considerably. Figure 2 shows the evolution of H_S (panel (a)) and θ (panel (b)) for the same 15 storms. The objective of the current work it to estimate a realistic model for storm trajectories such as those illustrated in Figure 1(b) and Figure 2.

[Figure 1 about here.]

[Figure 2 about here.]

3. MODEL

We estimate a model for the evolution of an interval I of time-series of consecutive values for threshold exceedances of sea state significant wave height, and corresponding direction $\{Y_t, \Theta_t\}_{t \in I}$, including the storm peak event (i.e. the occurrence of the largest value of H_S for the storm), sampled at some constant rate. For convenience, we assume time labels are centred such that for interval I, $t = 0 \in I$ corresponds to the time of the storm peak event. We estimate the model using a sample of m intervals $\{I_k\}$ of different lengths and data $\{\{y_{tk}, \theta_{tk}\}_{t \in I_k}\}_{k=1}^{m}$. The model is an extension of Markov extremal model of Winter and Tawn (2016, 2017), expressed for time-series on marginal standard Laplace scale. We therefore start the model description by outlining a non-stationary marginal model assumed applicable for all occurrences of H_S used to transform the sample of H_S values to standard Laplace scale.

3.1. Marginal modelling, transformation to Laplace scale and isolation of storm trajectories

We assume marginally that sea state significant wave height Y (for all intervals and all times regardless of magnitude) follows a two-part truncated gamma-generalised Pareto distribution (see Ross et al. 2017) with density

$$f_Y(y|\gamma,\zeta,\xi,\nu,\psi) = \begin{cases} \tau \times f_{TG}(y|\gamma,\zeta,\psi) \text{ for } y \leq \psi \\ (1-\tau) \times f_{GP}(y|\xi,\nu,\psi) \text{ for } y > \psi \end{cases}$$

where gamma shape γ and (inverse) scale ζ, generalised Pareto shape ξ and scale ν and threshold ψ are all functions of direction. In this work, ψ is estimated using non-stationary quantile regression prior to inference for gamma and generalised Pareto parameters, although in general ψ can be estimated as part of a single whole-sample inference as in Randell et al. (2016). Further

$$f_{TG}\left(y|\gamma,\zeta,\psi\right) = \frac{f_G\left(y|\gamma,\zeta\right)}{F_G\left(\psi|\gamma,\zeta\right)} \text{ for } y \in [0,\psi],$$

with gamma density

$$f_G\left(y|\gamma,\zeta\right) = \frac{\zeta^\gamma}{\Gamma(\gamma)} y^{\gamma-1} \exp\left(-\zeta x\right)$$

and generalised Pareto density

$$f_{GP}(y|\xi,\nu,\psi) = \frac{1}{\nu}\left(1+\frac{\xi}{\nu}\left(x-\psi\right)\right)^{-1/\xi-1} \quad .$$

Using F_Y to represent the estimated cumulative distribution function corresponding to density f_Y, we transform the sample to standard Laplace "X" scale using

$$X = \begin{cases} \log\left[2F(Y)\right] & \text{if } F(Y) < 1/2 \\ -\log\left[2\left\{1-F(Y)\right\}\right] & \text{otherwise .} \end{cases}$$

On Laplace scale, we identify storm intervals (and hence storm trajectories) as corresponding

to contiguous sequences of values of $X > \eta$ for some constant threshold η. Typical examples of the trajectories of the form $\{X_t, \Theta_t\}_{t \in I}$ isolated in this way are illustrated on physical scale (as $\{Y_t, \Theta_t\}_{t \in I}$) in Figure 1(b) and Figure 2 above, for η corresponding to the quantile of the standard Laplace distribution with non-exceedance probability 0.75 .

3.2. Markov extremal model for H_S

Winter (2015) describes a general k^{th}-order Markov extremal model `MEM(k)` for the evolution of time-series of extreme events on standard Laplace scale exceeding threshold η. In the current work, as justified in due course in Section 4, a second-order Markov extremal model (`MEM(2)`) is appropriate. We present this specific model here, as it is simpler to explain than a general k^{th}-order model, yet captures all the important features of `MEM(k)`. For the "post-peak" portion $\{X_t\}_{t \geq 0}$ of the time-series following the storm peak, model form is

$$[X_{t+1}, X_{t+2}] = [\alpha_1, \alpha_2]\, X_t + X_t^{[\beta_1, \beta_2]}\, [\mu_1 + \sigma_1 Z_1, \mu_2 + \sigma_2 Z_2] \text{ for } X_t > \eta$$

where $[Z_1, Z_2]$ is a dependent random variable, independent of X_t, with unknown distribution function $G_{1:2}$, where element-wise multiplication is assumed. Threshold η and parameters α_1, α_2, β_1, β_2 are taken to be constant. To estimate $[\alpha_1, \alpha_2]$ and $[\beta_1, \beta_2]$ we assume that

$$(X_{t+j} | X_t = x) \sim N\left(\alpha_j x + \mu_j x^{\beta_j}, \sigma_j^2 x^{2\beta_j}\right), \quad j = 1, 2$$

and then use the set of residuals from the fit in kernel density estimation (see Appendix) to estimate the joint distribution $G_{1:2}$ of $[Z_1, Z_2]$. Simulation under the model requires estimation of the conditional distribution $G_{2|1}$, which is also easily evaluated from the kernel density estimation. The basic simulation for $\{X_t\}_{t \geq 0}$ relative to the storm peak event X_0 proceeds as follows. First, a value for X_0 is sampled from the standard Laplace distribution. Then a realisation of the time-series of X_t is simulated using

$$\begin{aligned} X_1 &= \alpha_1 X_0 + X_0^{\beta_1}\, (\mu_1 + \sigma_1 Z_1), \text{ and} \\ X_t &= \alpha_2 X_{t-2} + X_{t-2}^{\beta_2} \left(\mu_2 + \sigma_2 Z_{2|1}\right) \text{ for } t = 2, 3, \ldots \end{aligned}$$

A similar procedure is used to estimate the corresponding model for the "pre-peak" portion $\{X_t\}_{t \leq 0}$, and simulate under it. Diagnostics for the choice of `MEM` order are discussed further

in Section 4.

3.3. Directional model

Exploratory analysis of the sample of directions $\{\theta_{tk}\}$ in Section 4 suggests that the rate of change of storm direction $d\Theta_t/dt$ when transformed empirically to marginal Gaussian scale as Δ_t ($= f(d\Theta_t/dt)$ for f estimated using the empirical cumulative distribution function and the probability integral transform) can be approximated using an order k autoregressive model (with $k = 1, 2, \dots$) according to

$$\Delta_t = \sum_{j=1}^{k} \gamma_j \Delta_{t-j} + \epsilon_t$$

with parameters $\{\gamma_j\}$, $\gamma_j \in [-1, 1]$, where ϵ_t is an additive error following a Gaussian distribution with variance dependent on the corresponding value of X_t

$$\epsilon_t \sim N\left(0, \sigma^2(X_t)\right)$$

and

$$\sigma^2(x) = \lambda_1 \exp(-\lambda_2 x) + \lambda_3 \quad .$$

The choice of functional form for σ^2 is motivated by the observation that there is little change in storm direction when the value of storm severity is high. A number of similar functional forms for σ^2 were examined in the application described in Section 4, with the form above providing good performance. Diagnostics for the choice of autoregressive model order are discussed further in Section 4.

3.4. Simulation under model

To generate a single "post-peak" storm trajectory using the fitted model, the simulation procedure is show below. An analogous approach is used to simulate the "pre-peak" trajectory.

simulate storm peak x_0, θ_0;
for $t = 1, 2, \ldots$ **do**
  simulate x_t using `MEM`;
  if $X_t \geq X_0$ **then**
    reject trajectory and restart;
  end
  if $X_t < \eta$ **then**
    stop and save trajectory;
  end
  simulate θ_t using directional model;
  simulate y_t on physical scale using marginal transformation;
end

Algorithm 1: Simulation scheme for "post-peak" storm trajectory.

4. APPLICATION

4.1. Marginal modelling and transformation to standard marginal scale

Using Bayesian inference, we estimate the non-stationary gamma-GP marginal model (Section 3.1) for the full sample of H_S, using a directional quantile threshold ψ corresponding to non-exceedance probability $\tau = 0.95$ illustrated effectively in Figure 1(a). Posterior median parameter estimates are illustrated in Figure 3 as thick solid lines. Figure 3 also shows parameter median estimates and 95% credible intervals for a generalised Pareto model of H_S^{sp} events exceeding the same directional quantile threshold ψ. Since consecutive values of H_S are dependent, we do not show credible intervals for parameters of the H_S model. Nevertheless, the credible intervals for H_S^{sp} model parameters give an indication as to the likely uncertainties in the H_S model parameters, since storm peak events are assumed independent.

[Figure 3 about here.]

Then we transform the full H_S sample from physical "Y" scale to standard Laplace marginal "X" scale using the median parameter estimates from the H_S model, and identify

contiguous intervals above a second (constant) threshold η corresponding to a non-exceedance probability of 0.75, thereby isolating a sample of storm trajectories. We examined the sensitivity of subsequent inferences to the choice of η and found these to be relatively stable.

4.2. Markov extremal model for H_S

For brevity in Section 4.2 and Section 4.3 below, we discuss and illustrate model estimates for the "pre-peak" portion of the storm trajectory only. Note that the corresponding analysis for the "post-peak" portion was also preformed, and exhibited similar characteristics to those discussed below. Both "pre-peak" and "post-peak" models are used in the simulation of storm trajectories in Section 4.4.

We consider a number of diagnostics for the Laplace-scale data, to judge an appropriate order k for the `MEM(k)` model to estimate. Figure 4(a) shows the partial autocorrelation function for X_t, indicating strong effects at lag 1 and 2, and potentially at larger lags also. Figure 4(b) shows estimates for the extremal dependence summary statistic χ (e.g. Eastoe et al. 2013) defined for time lag τ and threshold ω by

$$\chi(\tau, \omega) = \Pr\left(X_{t+\tau} > \omega | X_t > \omega\right) \quad .$$

The empirical estimate from the sample is shown in black. Other estimates are obtained from simulations under `MEM` models of different orders fitted to the sample. Inspection of Figure 4(b) suggests that `MEM(2)` provides a better description than `MEM(1)`, and that higher order models provide no additional benefit over `MEM(2)`.

[Figure 4 about here.]

Figure 5 shows scatter plots for pairs of parameter estimates for the `MEM(2)` model from a bootstrap resampling study.

[Figure 5 about here.]

4.3. Directional model for θ

Figure 6(a) shows the full sample of values for Δ_t on X_t, suggesting that Δ_t reduces with increasing X_t, and motivating the choice of directional autoregressive evolution variance in

Section 3.3. Figure 6(b) shows the partial autocorrelation function for Δ_t, indicating that only lag 1 is significant. We therefore proceed to fit an `AR(1)` model for Δ_t with non-stationary evolution variance $\sigma^2(X_t)$.

[Figure 6 about here.]

The estimated form of $\sigma^2(X_t)$ with X_t is illustrated in Figure 7 with 95% bootstrap uncertainty band, together with an empirical estimate direct from the sample.

[Figure 7 about here.]

4.4. Simulation under model and model validation

We use the simulation procedure from Section 3.4 to generate storm trajectories under the estimated non-stationary `MEM(2)` model. As indicated in Algorithm 1, the first step in the simulation would typically be to sample a realisation storm peak significant wave height and direction. This requires estimation of a model for the rate of occurrence of storm peak events in a given direction, and estimation of a model for the size of storm peak significant wave height given direction (the latter similar to that illustrated in Figure 3). In the current work, since focus is on estimation of storm evolution given storm peak, rather that estimating storm peak itself, we choose for clarity and simplicity to sample storm peak events with replacement from the historical sample of storm peaks rather than from a statistical model for storm peak characteristics.

Figure 4(b) and Figure 5 illustrate that the extremal dependence χ of simulated trajectories with lag agrees well with that of the original sample, and that non-stationary characteristics of the evolutionary variance of Δ_t are also in good agreement. Figure 8 shows 15 typical realisations in the same format as Figure 2; the characteristics of the trajectories in the two figures appear similar.

[Figure 8 about here.]

Further, we choose to examine whether the distribution of lengths of storm trajectories generated under the model are consistent with that of the original sample; this is of particular interest, since we do not explicitly seek to estimate storm length in the model from Section 3. Figure 9 illustrates this comparison for both `MEM(1)` and `MEM(2)` models. Agreement for the `MEM(2)` model is considerably better as might be expected.

[Figure 9 about here.]

Figure 10 compares the full distribution of sea state H_S from the original sample with that estimated from simulation under the `MEM(2)` model, in terms of the probability density function and the tail distribution. There is some suggestion that the mode of the body of simulated H_S is to the left to that of the original sample, but agreement is generally again good.

[Figure 10 about here.]

Figure 11 is a directionally-resolved version of Figure 9, comparing the distributions of storm lengths per directional octant. Figure 12 is a directionally-resolved version of Figure 10, comparing the distributions of H_S per directional octant. As in Figure 9 and Figure 10, agreement between simulations under the model and the original sample is good.

[Figure 11 about here.]

[Figure 12 about here.]

5. DISCUSSION AND CONCLUSIONS

We develop a non-stationary Markov extremal model (`MEM`) as an extension of Winter and Tawn (2016, 2017) and use it to characterise the time evolution of extreme sea state significant wave height (H_S) in the vicinity of the storm peak sea state. The approach first requires transformation of H_S from physical to standard Laplace scale, achieved using a non-stationary directional marginal extreme value model. The evolution of Laplace-scale H_S is subsequently characterised using a second-order `MEM`, and the evolution of rate of change of storm direction, transformed to Gaussian scale, is described by a first-order autoregressive model, the evolution variance of which is H_S-dependent. Simulations on the physical scale under the estimated model give realistic realisations of storm trajectories consistent with historical data, in terms of the distributions of trajectory lengths and total marginal distribution of H_S, at a northern North Sea location.

We consider the original `MEM` to be an important contribution to the environmental statistics and ocean engineering literature, since simple descriptions of the evolution of time-series

of extreme values of variables from the physical environment are needed in many contexts. Given that covariate effects are present in the majority of ocean engineering settings, we consider the current work to be a useful extension of `MEM`, allowing more realistic application in such settings. We note as obvious examples estimation of surge trajectories (e.g. Ross et al. 2018) for ocean storms, and characterisation of ocean current soliton events. The main motivation for the current work is the development of a statistical model to describe evolution of storm trajectories so that, given storm peak characteristics, realistic statistical simulators of storm evolution (as opposed to "storm matching" to events in a library of historical storms used in e.g. Feld et al. 2015) can be used for met-ocean design, thereby facilitating a more formal model-based uncertainty quantification.

There are many ways in which the current non-stationary model can be extended. In the current work we have assumed, given non-stationary marginal transformation to Laplace scale, that `MEM` parameters (on Laplace scale) are stationary with respect to covariate; we judge this to be a reasonable starting assumption supported by model diagnostics in the current application. However, in general we suspect that this may not always be the case, and that `MEM` parameters themselves may show covariate dependence. Keef et al. (2013) proposes additional constraints on the conditional extremes parameters which could be incorporated.

It would be interesting to consider the joint evolution of time-series of variables such as sea state H_S and spectral peak period T_P during a storm, non-stationary with respect to a common set of covariates; or joint modelling of time-series such as sea state H_S, wind speed and current speed with a much larger set of potential covariates. We might also consider the temporal evolution of storm trajectories jointly for multiple locations in a neighbourhood. The between-variable, between-time dependence structure of such a model would be interesting and probably challenging to identify.

ACKNOWLEDGEMENT

The acknowledge useful conversations with Graham Feld and Matthew Jones at Shell, and Jonathan Tawn at Lancaster University.

APPENDIX: ESTIMATION OF DISTRIBUTION OF MEM RESIDUALS

Following Section 3, for the "post-peak" portion $\{X_t\}_{t\geq 0}$ of the time-series following the storm peak, the second-order Markov extremal model form is

$$[X_{t+1}, X_{t+2}] = [\alpha_1, \alpha_2]\, X_t + X_t^{[\beta_1,\beta_2]}\, [\mu_1 + \sigma_1 Z_1, \mu_2 + \sigma_2 Z_2] \;\text{ for } X_t > \eta$$

where $[Z_1, Z_2]$ is a dependent random variable, independent of X_t, with unknown distribution function $G_{1:2}$, where element-wise multiplication is assumed. We write the full set of residuals available from the regression fit as $\{\hat{z}_{i1}, \hat{z}_{i2}\}_{i=1}^{n}$ where $\hat{z}_{ij} = (x_{t_i+j} - \hat{\alpha}_j x_{t_i} - \hat{\mu}_j x_{t_i}^{\beta_j})/(\hat{\sigma}_j x_{t_i}^{\beta_j})$, $j = 1, 2$ with $\{t_i\}$ representing the occurrence times of the corresponding observations of X, and $t = 0$ corresponding to the time of the storm peak. Then, following Winter (2015) we define kernel density estimates for the density g_1 of Z_1 and $g_{1,2}$ of $[Z_1, Z_2]$ as

$$g_1(z_1) = \frac{1}{n}\sum_i \frac{1}{h_1} f\left(\frac{z_1 - \hat{z}_{i1}}{h_1}\right)$$

and

$$g_{1,2}(z_1, z_2) = \frac{1}{n}\sum_i \frac{1}{h_1 h_2} f\left(\frac{z_1 - \hat{z}_{i1}}{h_1}\right) f\left(\frac{z_2 - \hat{z}_{i2}}{h_2}\right)$$

where f is the kernel density, taken in this work to be Gaussian, and (h_1, h_2) are kernel widths estimated by inspection of resultant estimates for densities g_1 and $g_{1,2}$. Then the cumulative distribution function $G_{2|1}$ of the conditional residual $Z_{2|1}$ can be written

$$G_{2|1}(z_2|z_1) = \sum_i w_i(z_1) F\left(\frac{z_2 - \hat{z}_{i2}}{h_2}\right)$$

where F is the kernel cumulative distribution function corresponding to density f, and weights $\{w_i(z_1)\}$ are given by

$$w_i(z_1) = \left(\sum_{i'} f\left(\frac{z_1 - \hat{z}_{i'1}}{h_1}\right)\right)^{-1} f\left(\frac{z_1 - \hat{z}_{i1}}{h_1}\right) \quad .$$

REFERENCES

Chavez-Demoulin, V., Davison, A., 2012. Modelling time series extremes. Revstat 10, 109–133.

Davison, A. C., Padoan, S. A., Ribatet, M., 2012. Statistical modelling of spatial extremes. Statist. Sci. 27, 161–186.

Eastoe, E., Koukoulas, S., Jonathan, P., 2013. Statistical measures of extremal dependence illustrated using measured sea surface elevations from a neighbourhood of coastal locations. Ocean Eng. 62, 68–77.

Feld, G., Randell, D., Ross, E., Jonathan, P., 2018. Design conditions for waves and water levels using extreme value analysis with covariates. (Submitted to Ocean Engineering, draft at www.lancs.ac.uk/∼jonathan).

Feld, G., Randell, D., Wu, Y., Ewans, K., Jonathan, P., 2015. Estimation of storm peak and intra-storm directional-seasonal design conditions in the North Sea. J. Offshore. Arct. Eng. 137, 021102:1–021102:15.

Heffernan, J. E., Tawn, J. A., 2004. A conditional approach for multivariate extreme values. J. R. Statist. Soc. B 66, 497–546.

Huser, R., Davison, A. C., 2014. Space-time modelling of extreme events. J. Roy. Statist. Soc. B 76, 439–461.

Keef, C., Papastathopoulos, I., Tawn, J. A., 2013. Estimation of the conditional distribution of a vector variable given that one of its components is large: additional constraints for the Heffernan and Tawn model. J. Mult. Anal. 115, 396–404.

Padoan, S. A., Ribatet, M., Sisson, S. A., 2010. Likelihood - based inference for max - stable processes. J. Am. Statist. Soc. 105, 263–277.

Randell, D., Turnbull, K., Ewans, K., Jonathan, P., 2016. Bayesian inference for non-stationary marginal extremes. Environmetrics 27, 439–450.

Reich, B. J., Shaby, B. A., 2012. A hierarchical max-stable spatial model for extreme precipitation. Ann. Appl. Stat. 6, 1430–1451.

Reistad, M., Breivik, O., Haakenstad, H., Aarnes, O. J., Furevik, B. R., Bidlot, J.-R., 2011. A high-resolution hindcast of wind and waves for the North sea, the Norwegian sea, and the Barents sea. J. Geophys. Res. 116, 1–18.

Rootzen, H., Segers, J. L., Wadsworth, J., 2018. Multivariate peaks over thresholds models. Extremes 21, 115–145.

Ross, E., Randell, D., Ewans, K., Feld, G., Jonathan, P., 2017. Efficient estimation of return value distributions from non-stationary marginal extreme value models using Bayesian inference. Ocean Eng. 142, 315–328.

Ross, E., Sam, S., Randell, D., Feld, G., Jonathan, P., 2018. Estimating surge in extreme North Sea storms. Ocean Eng. 154, 430–444.

Stephenson, A., 2009. High-dimensional parametric modelling of multivariate extreme events. Aust. N. Z. J. Stat. 51, 77–88.

Wadsworth, J. L., Tawn, J. A., Davison, A. C., Elton, D. M., 2017. Modelling across extremal dependence classes. J. Roy. Statist. Soc. C 79, 149–175.

Winter, H. C., 2015. Extreme value modelling of heatwaves. PhD thesis, Lancaster University, U.K.

Winter, H. C., Tawn, J. A., 2016. Modelling heatwaves in central France: a case-study in extremal dependence. J. Roy. Statist. Soc. C 65, 345–365.

Winter, H. C., Tawn, J. A., 2017. kth-order Markov extremal models for assessing heatwave risks. Extremes 20, 393–415.

FIGURES

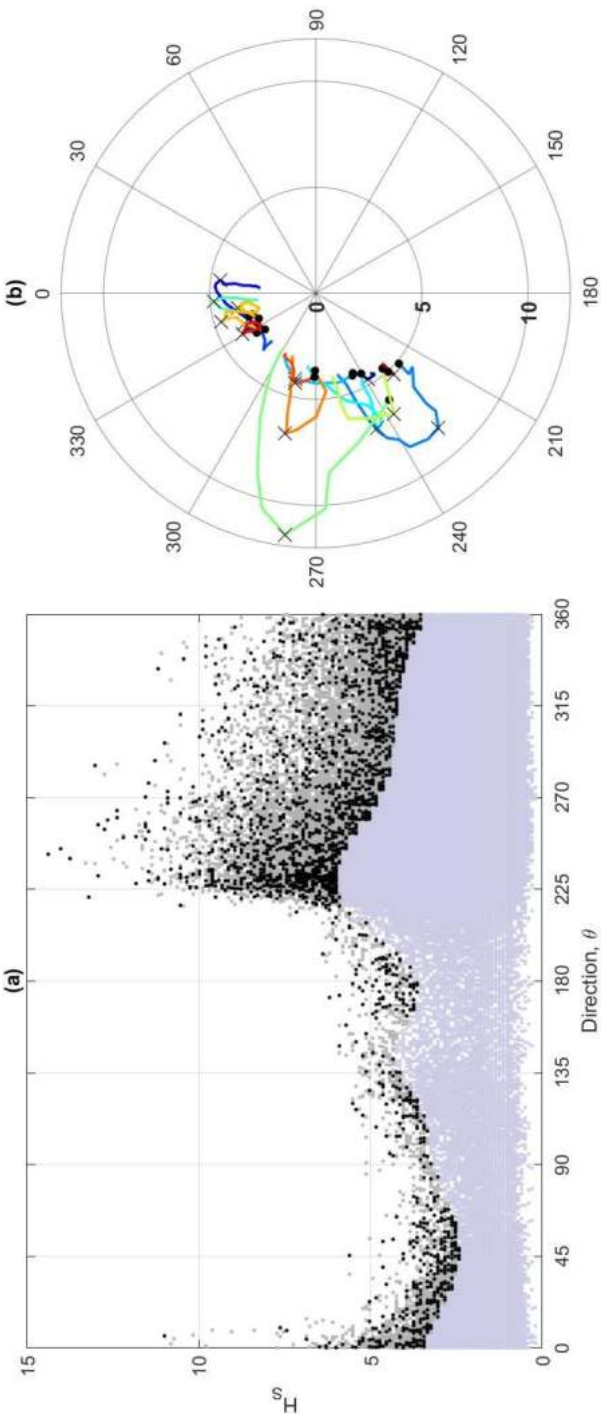

Figure 1. Motivating application. (a) Directional plot of storm peak H_S (black) and (sea state) H_S (grey) for all storms. (b) Polar plot of H_S trajectories with direction for 15 typical storms.

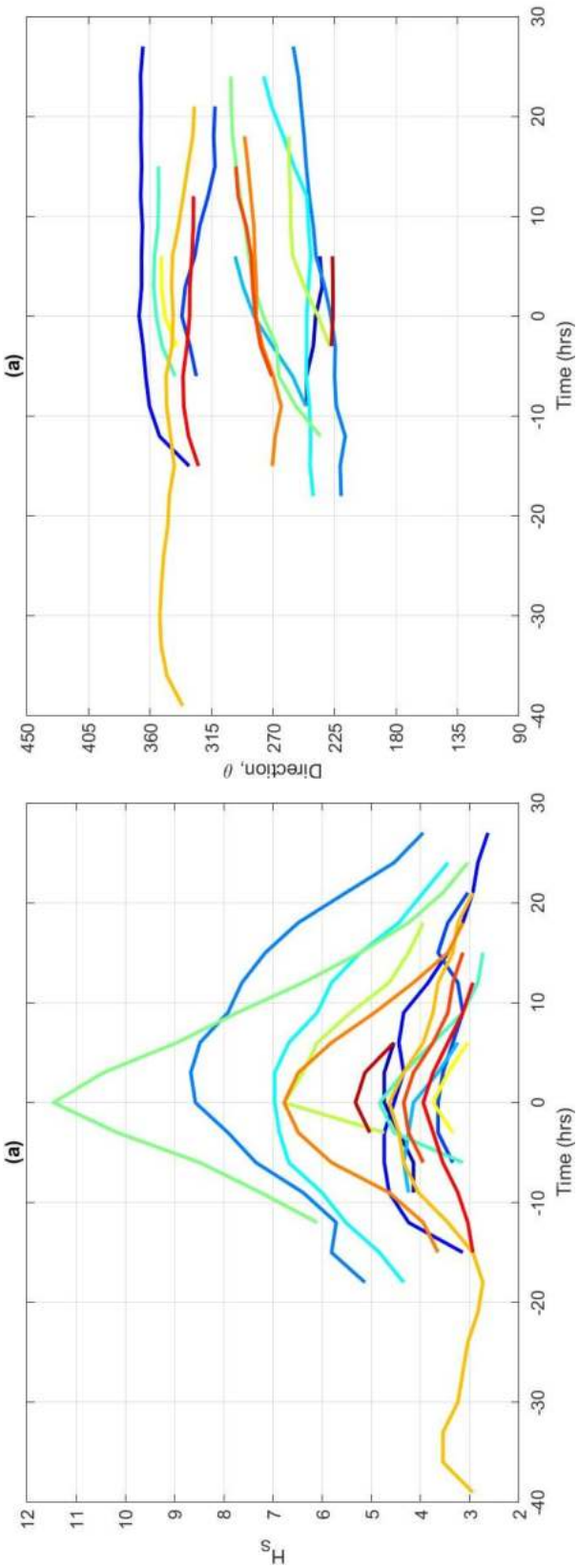

Figure 2. Time evolution for the 15 typical storms (shown also in Figure 1). (a) H_S in time. (b) θ in time.

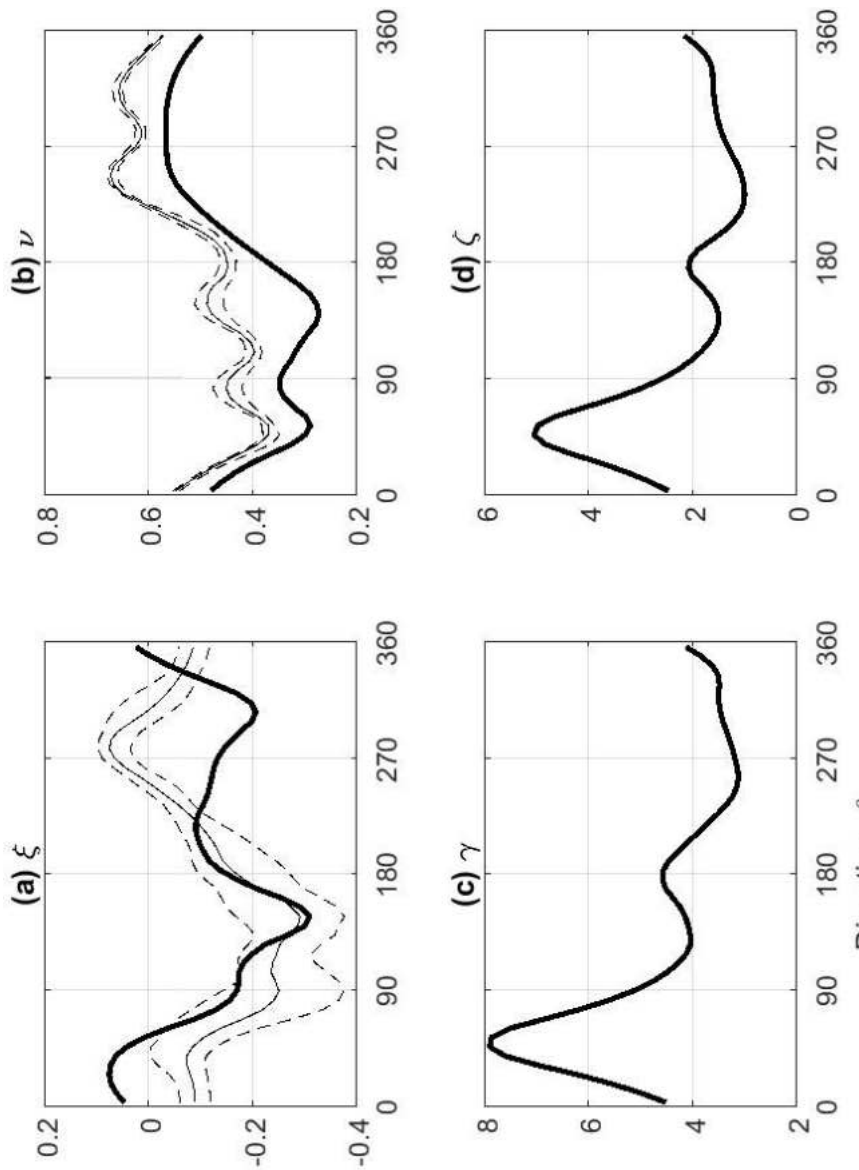

Figure 3. Parameter estimates ξ, ν, γ and ζ for the directional marginal gamma-GP model for sea state significant wave height H_S and storm peak significant wave height H_S^{sp}. Thick solid lines are median parameter estimates for H_S. Thin solid lines are median estimates for H_S^{sp}. Thin dashed lines are 95% uncertainty bands for H_S^{sp}. The directional threshold ψ used is illustrated in Figure 1.

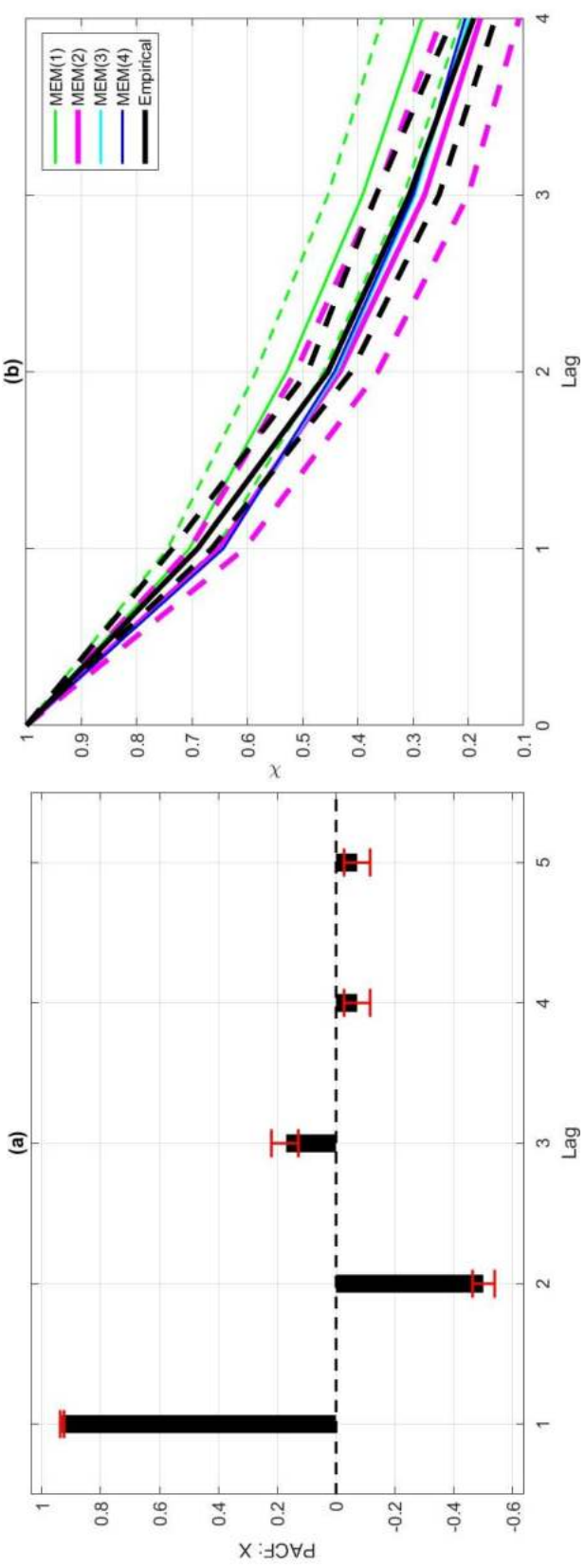

Figure 4. Choice of model order for Markov extremal model of Laplace-scale $H_{S\dagger}$, X. (a) Sample partial auto-correlation function, with bootstrap 95% uncertainty bands in red. (b) Tail summary statistic χ corresponding to a non-exceedance probability of 0.995 for the sample and for realisations under models of different orders. 95% bootstrap uncertainty bands are shown for the original sample (black), `MEM(1)` (green) and `MEM(2)` (pink) only. Uncertainty bands for `MEM(3)` and `MEM(4)` estimates have similar widths to those of `MEM(2)`, and are omitted for clarity.

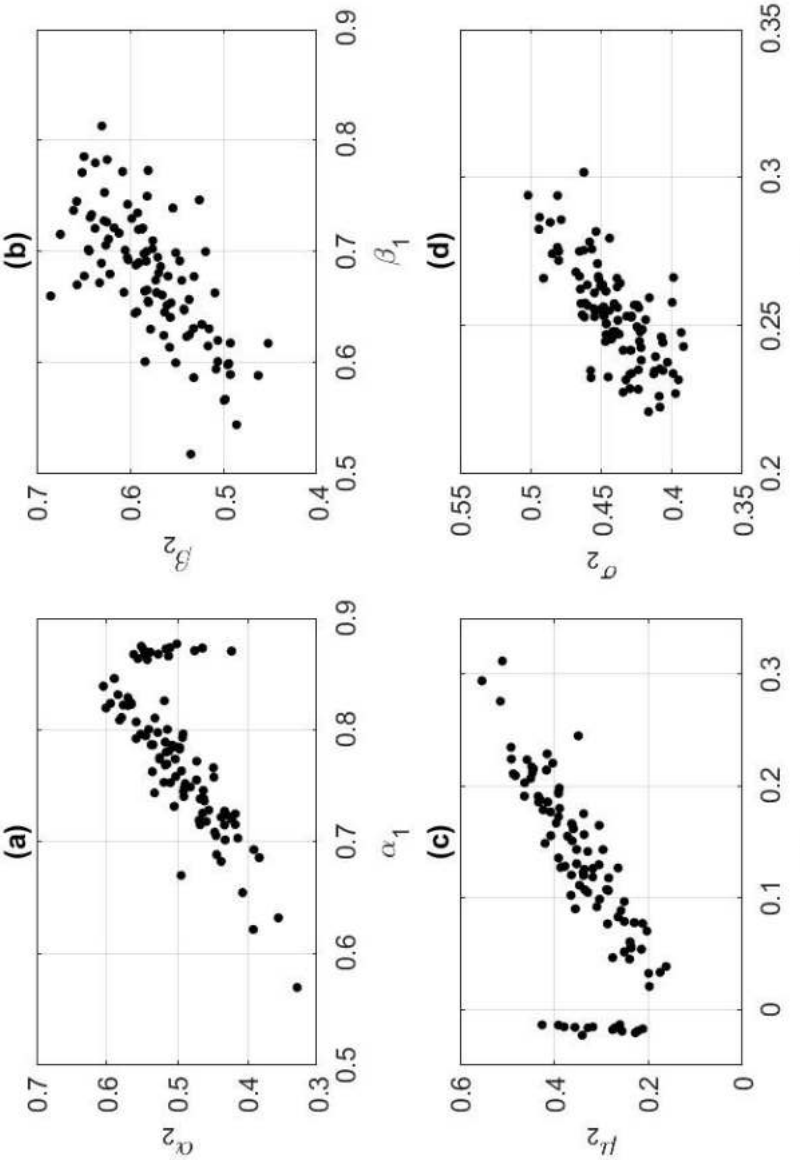

Figure 5. Scatter plots of α_2 on α_1, β_2 on β_1, μ_2 on μ_1 and σ_2^2 on σ_1^2 for `MEM(2)` pre-peak model for H_S from a bootstrap resampling analysis, using a threshold with non-exceedance probability 0.75 .

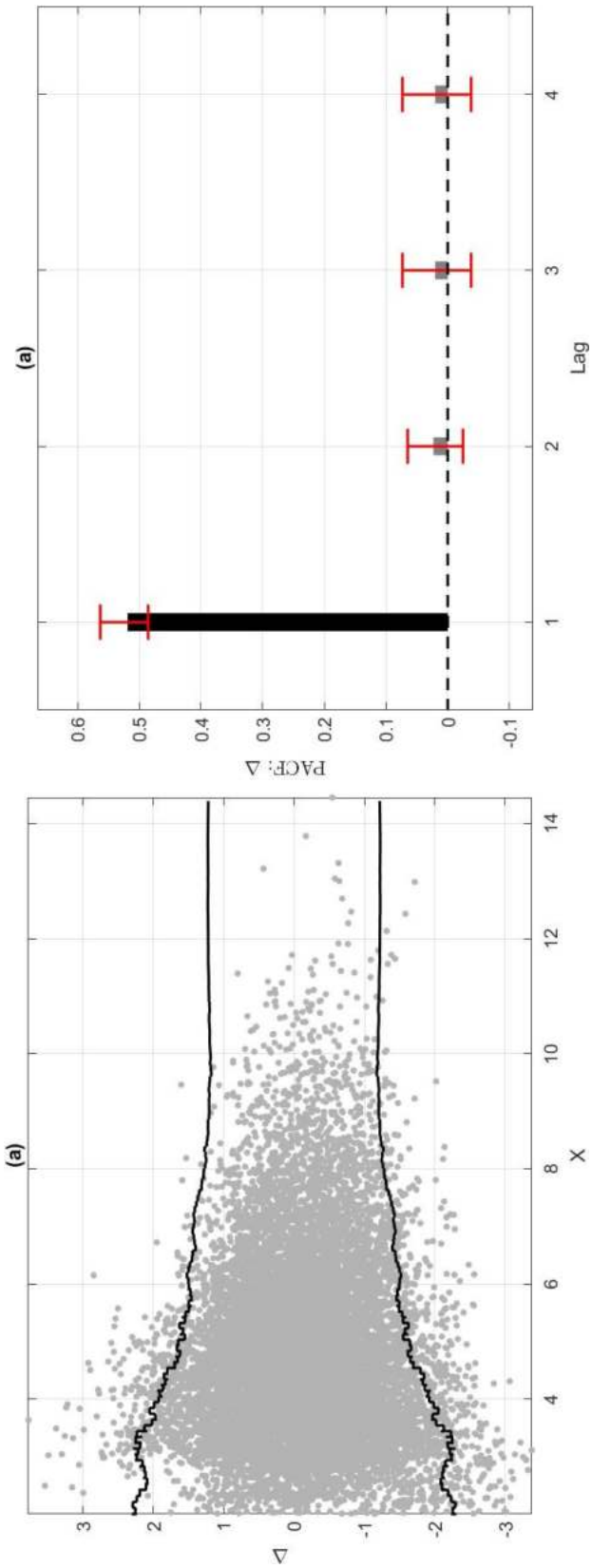

Figure 6. Directional diagnostics. (a) Δ_t on X_t from sample. (b) Sample partial autocorrelation function for Δ_t with bootstrap 95% uncertainty bands in red.

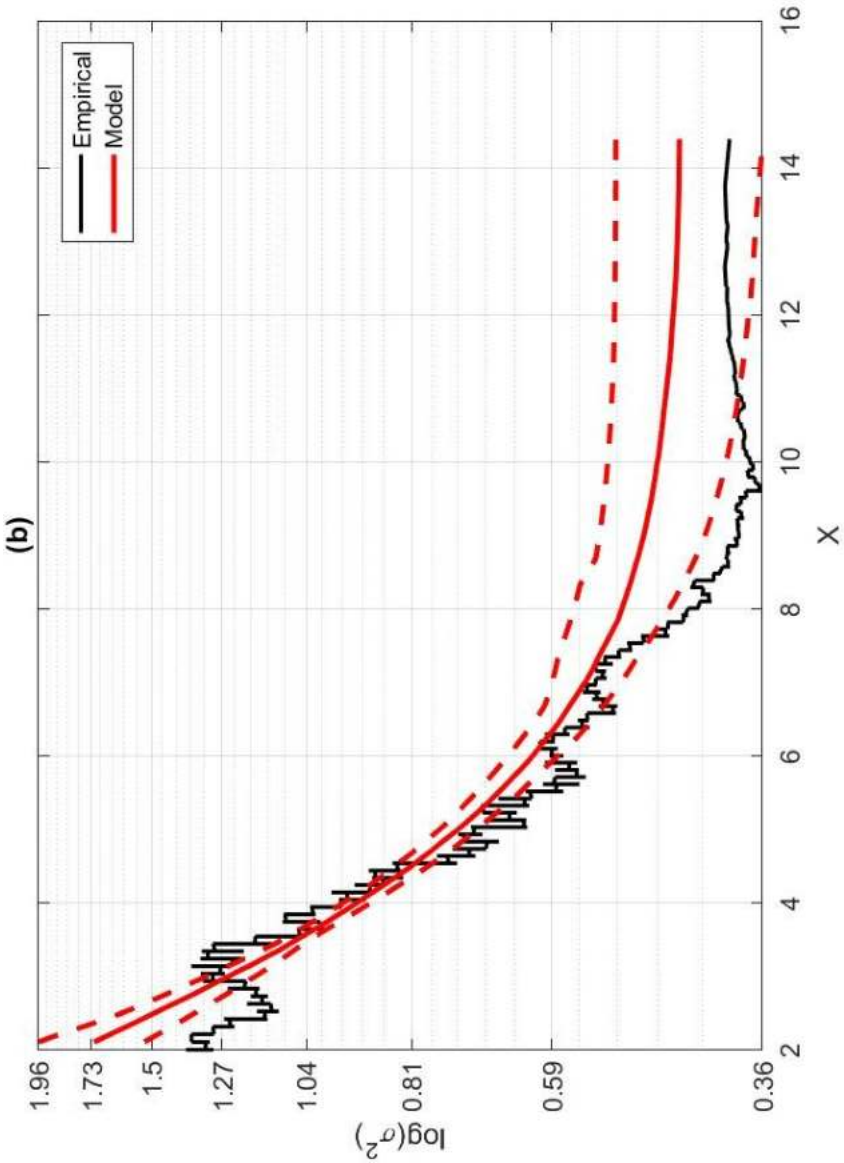

Figure 7. Directional model. Empirical (black) and model estimates (red, with 95% bootstrap uncertainty band) for decay of $\sigma^2(X_t)$ with X_t.

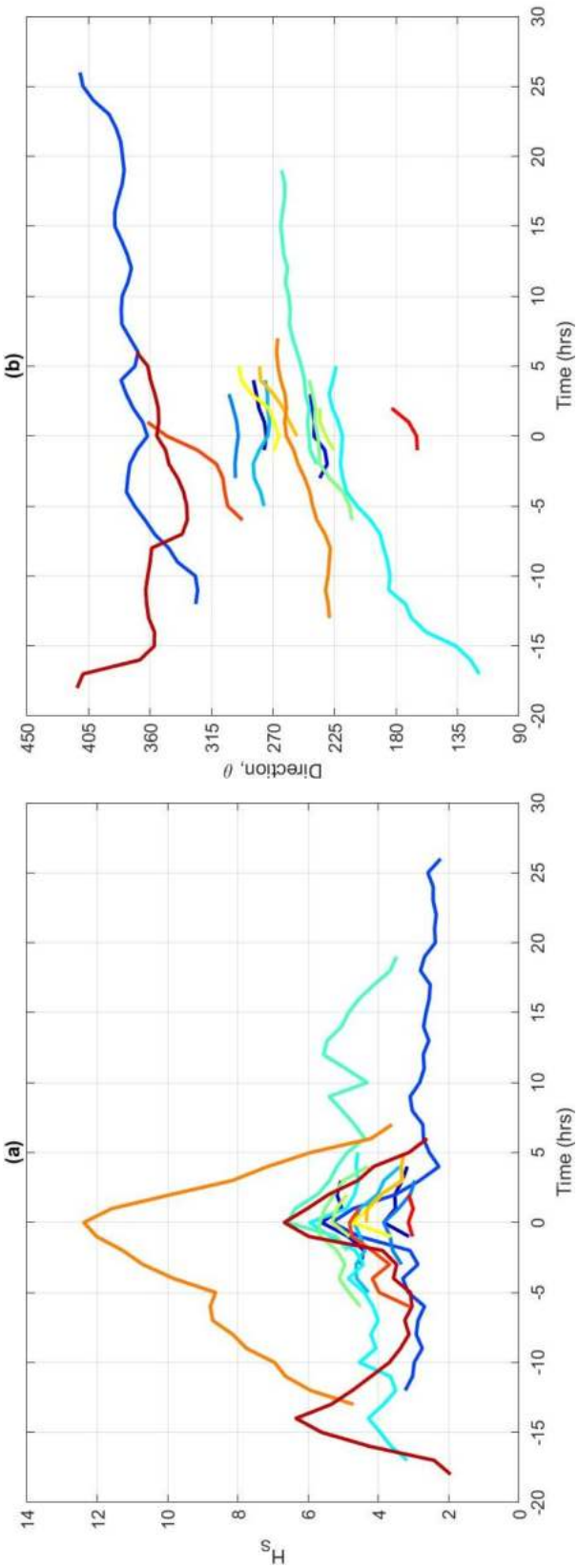

Figure 8. Time evolution of 15 typical realisations of storm trajectories. (a) H_S in time. (b) θ in time.

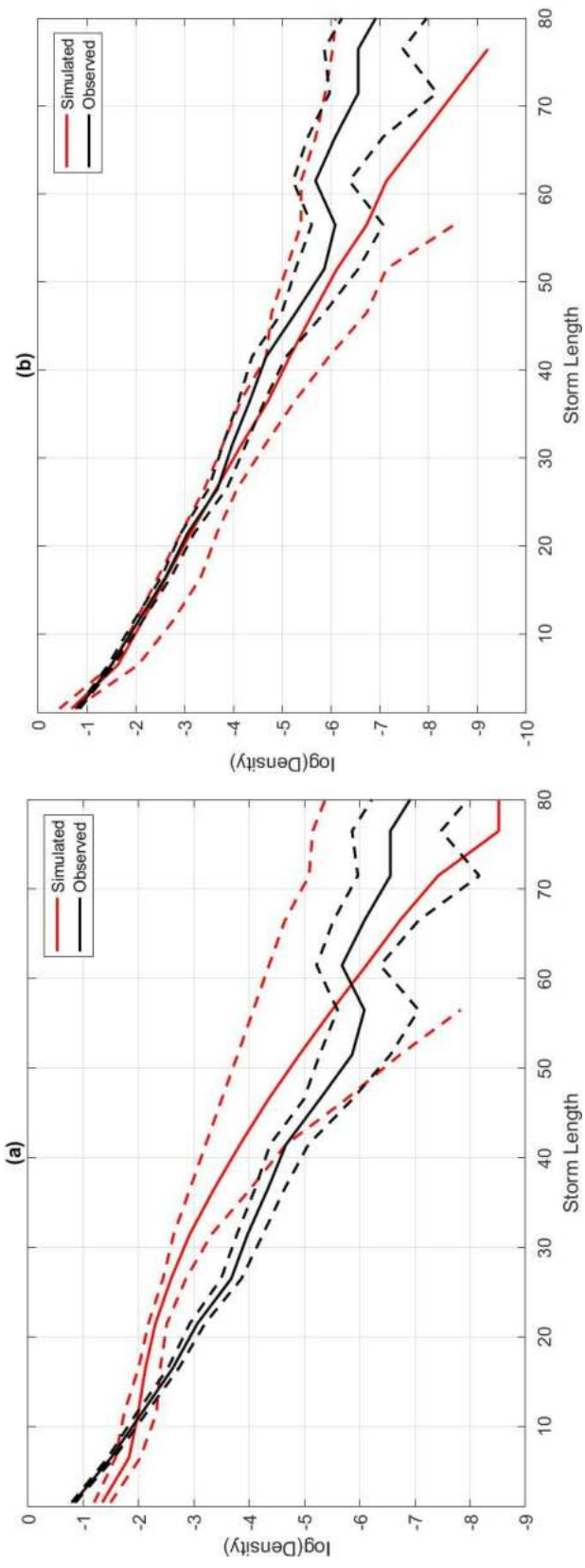

Figure 9. Logarithm of the density of number of sea states in a storm with first order directional model and (a) `MEM(1)` and (b) `MEM(2)`. Black lines give empirical sample estimates with 95% bootstrap uncertainty band. Red lines are estimated by simulation under the model.

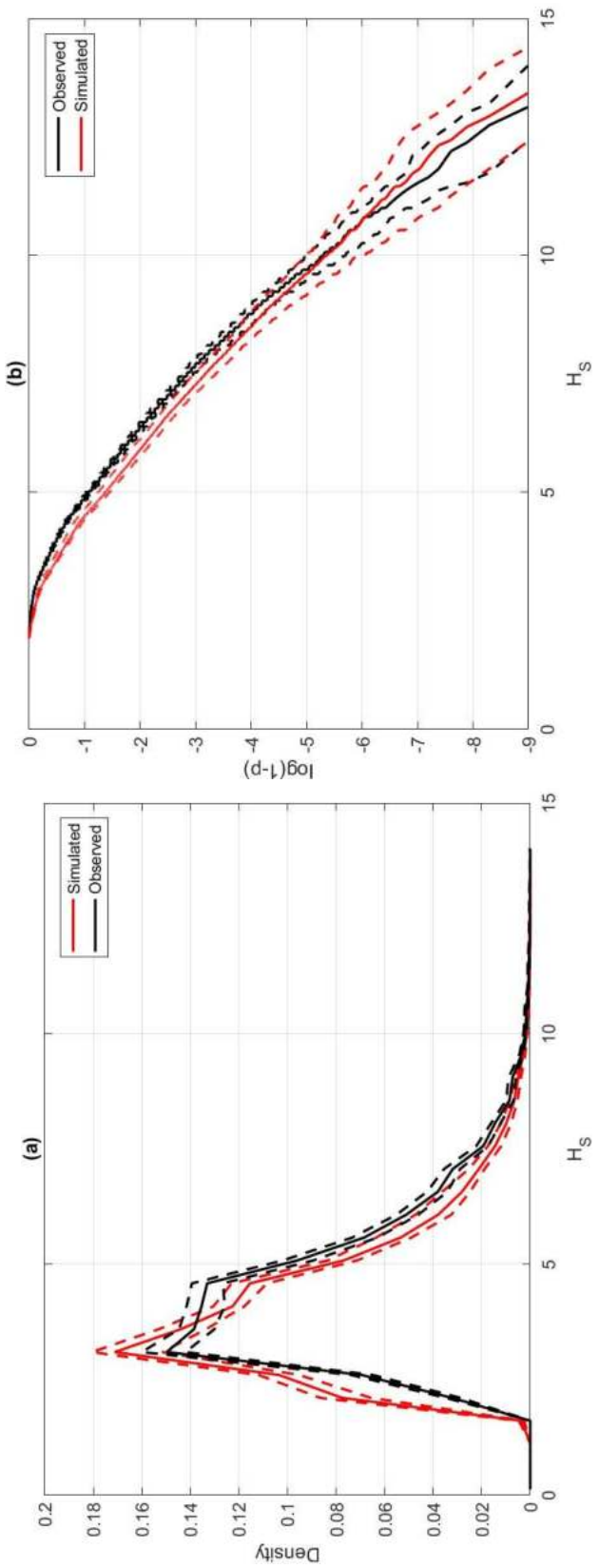

Figure 10. Comparison of distribution of H_S from sample (black) and simulation under fitted `MEM(2)` model (red) with 95% bootstrap uncertainty bands. (a) Density. (b) Tail of distribution.

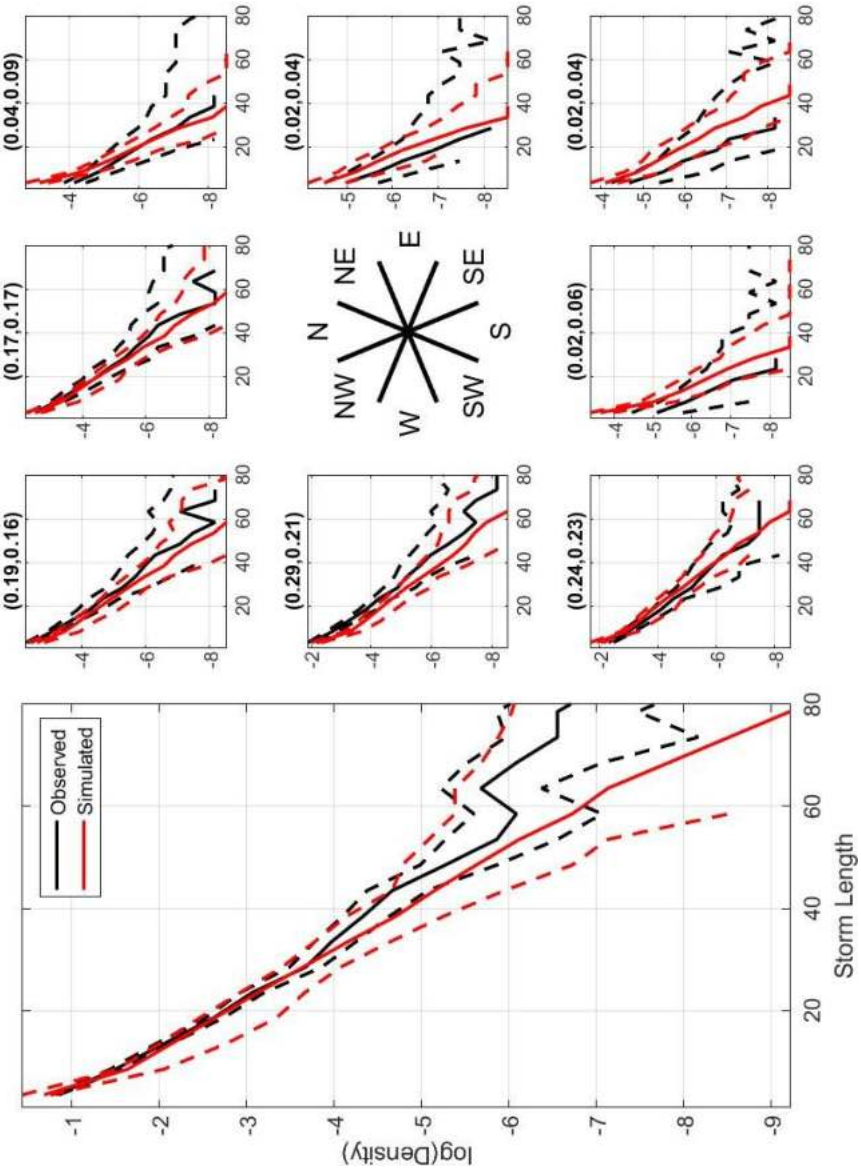

Figure 11. Directional comparison of logarithm of density of storm lengths. The left hand panel shows the omni-directional comparison, and the smaller plots show comparisons for 8 directional octants centred on cardinal and inter-cardinal directions. Each panel shows original sample tail (black) and simulated tail (red) with 95% bootstrap uncertainty bands. Titles of smaller panels give the percentage of storm peak occurrences in the directional octant, first from the original sample and then from simulation.

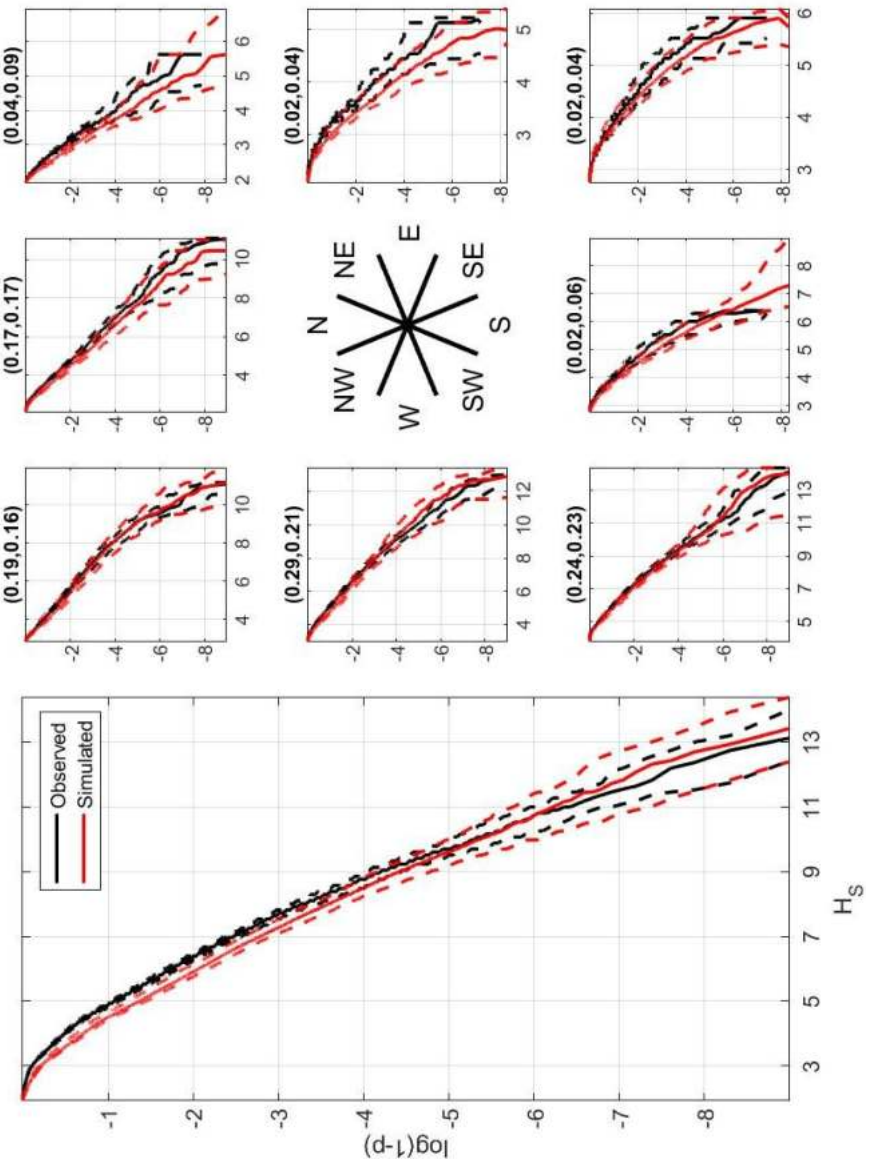

Figure 12. Directional comparison of tails of distributions of H_S. The left hand panel shows omni-directional comparison, and the smaller plots show comparisons for 8 directional sectors centred on cardinal and inter-cardinal directions. Each panel shows original sample tail (black) and simulated tail (red) with 95% bootstrap uncertainty bands. Titles of smaller panels give the percentage of storm peak occurrences in the directional octant, first from the original sample and then from simulation.